

Microstructure-conductivity correlation for hot-pressed 8YSZ powders

J. Van herle ^{a,*}, R. Vasquez Cavieres ^a, D. Akyuz ^b, K. Barthel ^c

^aFederal Institute of Technology EPFL, DC-LPI, 1015 Lausanne, Switzerland

^bFederal Institute of Technology EPFL, DMX-LTP, 1015 Lausanne, Switzerland

^cFederal Laboratory for Materials Testing and Research (EMPA), 3602 Thun, Switzerland

Received 4 September 2000; received in revised form 6 November 2000; accepted 18 December 2000

Abstract

Coarse 8YSZ powders destined for plasma spray deposition were obtained from three different suppliers (Hochrhein, Magnesium Elektron, Unitec). Their ionic conductivities were measured by impedance spectroscopy on pellets prepared by vacuum hot pressing. Density was adequate for one powder (Unitec, 95%) but poor for the other two (73–80%). For the latter samples, conductivity was a factor of 1.5 below reference values for pure dense 8YSZ, owing to their porosity. For the former samples, however, the conductivity was a factor >3 below 8YSZ reference values. An additional resistance, responsible for this large discrepancy, appeared in the impedance response and is ascribed to the distinct microstructure at intergranular zones within these otherwise dense samples. © 2001 Published by Elsevier Science Ltd. All rights reserved.

Keywords: Hot pressing; Impedance; Ionic conductivity; Microstructure-final; Sintering

1. Introduction

Plasma spraying (PS) is considered as one of the fabrication techniques for solid oxide fuel cells (SOFC). Several groups in Japan and Europe have used it extensively^{1–4} because of its promise of ease of automation for manufacturing large quantities of samples. A difficulty resides in fabricating dense layers for the yttria-stabilized zirconia (YSZ) fuel cell electrolyte. This is related to the fact that coarse starting powders, 20–30 μm in grain size, have to be employed. Finer powders will block the spraying nozzle or volatilize upon spraying, thus involving large material loss. The layered deposit after spraying will retain a relatively coarse structure, with voids that affect conductivity⁵ that causes gas leakage during fuel cell operation. The choice of the starting powder for plasma spray application, therefore, requires special attention including grain size and shape. This work examined the conductivity behaviour of PS powders of different origin. We previously characterised as-sprayed YSZ layers but encountered

technical limitations for reliable determination of the conductivity.⁵ The powders were here compacted to thick pellets, allowing for more accurate conductivity measurements.

2. Experimental

Three PS powders of 8 mol% $\text{Y}_2\text{O}_3\text{--ZrO}_2$ were obtained from three suppliers: Hochrhein (D, HR), Magnesium Elektron (UK, MEL) and Unitec (UK, U). They were sintered by vacuum hot pressing at 1400°C (4 h) in Ar atmosphere to discs 30 mm in diameter and 3 mm thick. The discs were given a re-oxidation treatment in air for 2 h at 1000°C (samples labeled as HR1000, MEL1000, U1000) and 1500°C (samples labeled as HR1500, MEL1500, U1500). Densities were determined by the Archimedes method. Silver paint was applied over 4 cm^2 symmetrically on both faces of each pellet. Platinum mesh with platinum leads was contacted to the electrodes and thermocompressed in air at 800°C. Four-Point conductivity measurements on each sample were carried out between 200 and 900°C using impedance spectroscopy. The frequency range was 0.1–1 MHz. Data analysis was performed by equivalent electrical circuit fitting (Zahner Elektrik, D, Model IM6).

* Corresponding author. Tel.: +41-21-693-5754; fax: +41-21-693-4111.

E-mail address: jan.vanherle@epfl.ch (J. Van herle).

For comparison, a pellet was uniaxially compacted from fine 8YSZ powder prepared in-house by a coprecipitation method. After sintering at 1400°C in air, final density of 99% was achieved. The ionic conductivity in air of this sample served as reference values.

3. Results

The impurity content of the supplied powders was fairly low and showed but small differences among them. These are given in Table 1 together with the sample densities obtained. Two powders compacted poorly (Hochrhein, Magnesium Elektron) to give 80 and 73% relative density, while the other powder (Unitec) sintered to reasonable density (94–97%). No influence on final density was observed when resintering the samples at 1500°C rather than 1000°C.

Examples of the microstructures are given in Figs. 1 and 2. Fig. 1a shows a scanning electron micrograph (SEM) of the starting powder from Hochrhein, and Fig. 2a of the fracture surface of the sintered sample HR1500. Fig. 1a shows coarse broken particles of several 10 µm in size, which reappear in the sintered structure of Fig. 2a. An identical result was obtained for MEL powder and samples.

Fig. 1b shows a SEM of the Unitec starting powder and Fig. 2b of the fracture surface of the sintered sample U1000. This powder distinguishes itself from the other two by a more spherical shape of agglomerates composed of micron-sized particles. After sintering, two morphologies appear (Fig. 2b): regions showing full densification and those showing the original smaller particles. A close-up is displayed in Fig. 2c.

Examples of the impedance response are given in Fig. 3. Fig. 3a shows a result for sample HR1000, at 352°C. A classical response is observed⁶ of a large semicircle at high frequency, corresponding to the intragrain resistance, and a smaller one at intermediate frequency, corresponding to the grainboundary resistance. The last arc, at lowest frequency, represents the silver electrode response. It was always included in the fitting procedure in order to properly deconvolute the grainboundary resistance. Impedance results on Magnesium Elektron samples and the reference 8YSZ pellet appeared very similar to those

on the Hochrhein samples. Both intragrain and grain boundary semicircles could be well deconvolved up to 400°C, between 400 and 550°C only the grain boundary response was determined (the bulk resistance being the intersection value with the real axis), and from 600°C onwards only the silver electrode response appeared, where the high frequency intercept indicated the total 8YSZ resistance.

Fig. 3b shows the impedance result for sample U1000, at 315°C. A large additional semicircle appears at frequencies between the intragrain and grain boundary responses and dominates the total resistance into high temperatures.

4. Discussion

From impedance analysis, resistance values for the intragrain, grainboundary and the additional arc (Unitec samples) were obtained and normalised to resistivity by taking account of the geometry. This simple treatment applies for intragrain values and gives only apparent values for the grainboundary behaviour but was adopted for ease of comparison. These resistivity values were plotted on Arrhenius graphs, from which line fits were calculated in limited temperature regimes.

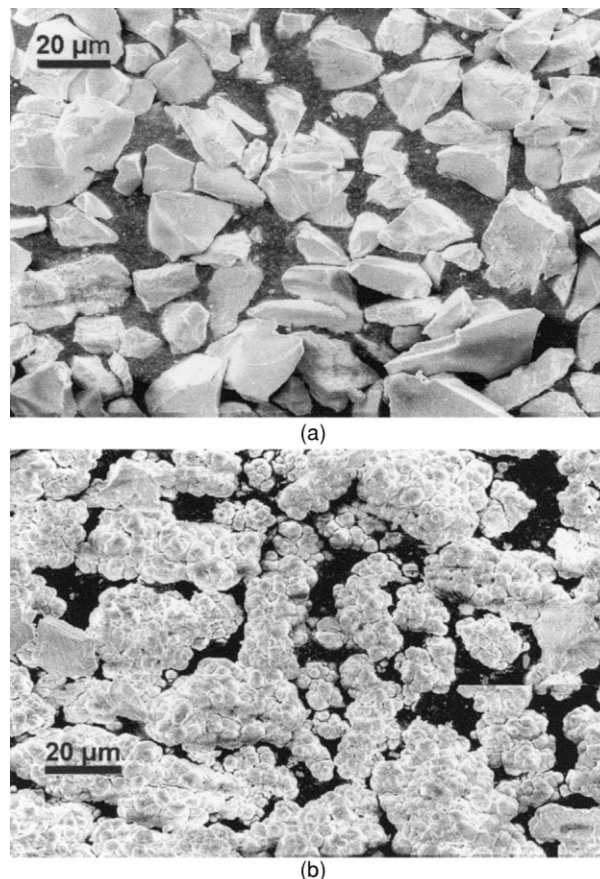


Fig. 1. SEM (1000×) of (a) Hochrhein powder, (b) Unitec powder.

Table 1
Impurity of 8YSZ PS powders and obtained density of hot pressed samples

Sample	HR1000	HR1500	MEL1000	MEL1500	U1000	U1500
Rel. density (%)	81.0	79.5	73.0	73.5	97.4	94.5
Impurity wt.% Si	0.02		0.04		0.025	
Ti	0.20		0.09		0.12	
Al	0.25		0.01		0.04	
Fe	0.01		0.10		0.02	
Na					0.10	

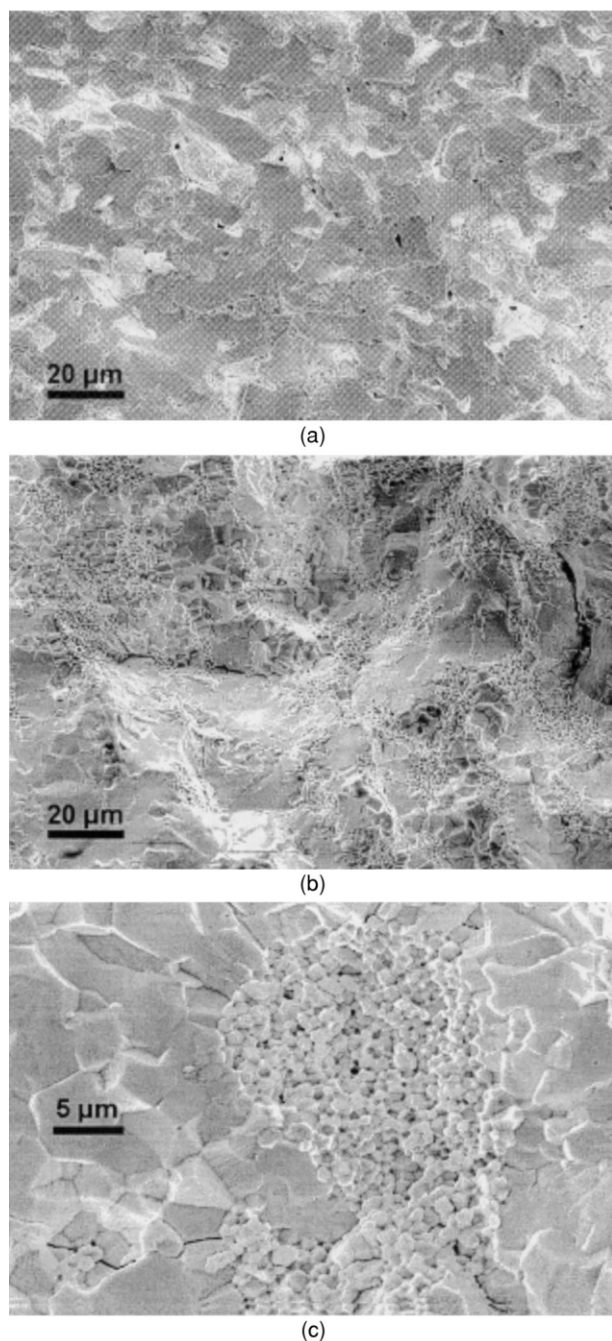


Fig. 2. SEM (1000 \times) of fracture surface of sample (a) HR1500 (Hochrhein), (b) U1500 (Unitec), (c) SEM (4000 \times) of fracture surface of sample U1500 (Unitec), close-up.

The fits allowed to interpolate values at selected temperatures, to compare the different samples. The results are summarised in Tables 2 and 3.

Table 2a displays individual resistivities for HR samples and Table 2b for Unitec samples. Table 3 compares the total resistivities of the samples HR1500, MEL1500 and U1500 with those of the reference 8YSZ pellet.

Values for intragrain (R_{ig}) and grain boundary (R_{gb}) resistivity $\geq 600^\circ\text{C}$ are extrapolated from low tempera-

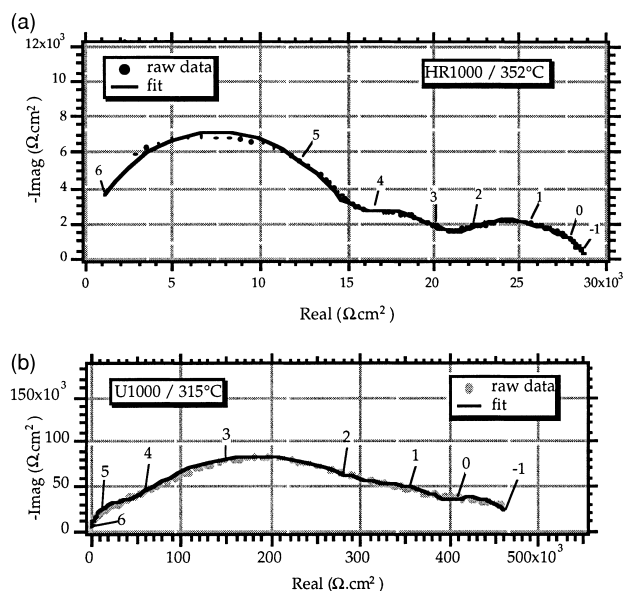


Fig. 3. Impedance spectrum of conductivity response of sample (a) HR1000 in air, at 352°C ; (b) U1000 air, at 315°C . Numbers indicate frequencies in powers of 10 Hz.

ture fits. For these temperatures, they sum up to lower total resistivities than those obtained experimentally (R_{tot}). This originates from a decreasing activation energy at higher temperatures.⁷ Hence, only the R_{tot} columns in Tables 2 and 3 are relevant for high temperatures.

Samples HR1500 and MEL1500 approach the conductivity behaviour of the reference 8YSZ sample. At high temperature, of relevance for SOFC application, they differ by less than 50%, which can be accounted for by their high porosity. The difference between samples MEL1000 and MEL1500 was marginal (10%), but that between HR1000 and HR1500 quite significant (factor 2). The re-annealing step at 1500°C showed the beneficial effect of improving the intragrain conductivity of HR samples. This can be due to improved densification or dissolution of impurities. It is unclear which has prevailed in the present case. Densities and SEM observation for samples HR1000 and HR1500 were similar and impurity concentrations (Table 1) seem sufficiently low. Ti and Al concentrations in HR powder were indeed slightly higher than with MEL, and Ti impurity increases the grain boundary resistance.⁸ In conclusion, useful conductivity for HR samples was obtained only after a high temperature reannealing step.

Samples U1000 and U1500, despite good density, differ largely from expected conductivity values. Reannealing at 1500°C did not change the intragrain behaviour, but lowered the other two resistive terms for a total conductivity improvement by 50%. This still remained well below 8YSZ reference values (factor of 3) at SOFC temperatures. The most marked feature is the dominating extra semicircle (Fig. 3b). It seems unlikely

Table 2

Interpolated intragrain resistivity and apparent grain boundary resistivity of Hochrhein and Unitec samples

T (°C)	Sample HR1000			Sample HR1500		
	R_{ig}	R_{gb}	R_{tot}	R_{ig}	R_{gb}	R_{tot}
Ω (cm ²)						
(a) Hochrhein samples						
300	223,683	201,282	424,964	266,089	124,008	390,097
400	12,814	6271	19,085	12,687	4517	17,204
500	1568	489	2057	1355	395	1751
600	315	69	500	245	61	309
700	89	15	157	64	14	83
800	32	4.3	62	21.5	4.3	28.9
900			28.9			12.1

T (°C)	Sample U1000				Sample U1500			
	R_{ig}	R_{gb}	R_{void}	R_{tot}	R_{ig}	R_{gb}	R_{void}	R_{tot}
Ω (cm) ²								
(b) Unitec samples								
300	334k	5745k	996k	1906k	204k	293k	590k	1088k
400	17,350	19,176	51,169	87,694	12,579	10,435	33,982	56,996
500	1971	1572	5776	9319	1625	897	4174	6696
600	374	232	1091	1697	340	137	841	1189
700	101	51	293	396	100	31	238	267
800	35.2	15.2	101.9	118.8	37.0	9.5	86.3	79.8
900							44.1	29.6

that Unitec powder impurities are responsible for the large effect observed, given the contrary evidence with HR and MEL samples, whose impurity content is similar to that of Unitec but which showed lower and acceptable resistivities. From microstructural evidence of Fig. 2b and c, it seems plausible to attribute this extra term to the disrupted regions dispersed throughout the sample body, that consist of many small grains. Evidence of an extra semicircle in impedance response being due to voids or bad contacts at grains has been explained as charge carriers accumulating at these bottlenecks.^{9,10} This extra resistive term has, therefore, been referred to as “ R_{void} ” in Table 2b.

5. Conclusion

Coarse 8YSZ powders for SOFC plasma spraying were compacted to pellets to assess their conductivity behaviour. Samples from Hochrhein and Magnesium Elektron, despite final density of 73–80%, showed reasonable values, 20–50% lower than fully dense reference 8YSZ at SOFC temperatures. Hochrhein samples required re-annealing at high temperature (1500°C) to obtain this result. Samples from Unitec, despite final density of 95%, showed much lower conductivity than reference 8YSZ, by a factor 3, even after re-annealing. A dominating extra resistance was evident from impe-

Table 3

Interpolated intragrain resistivity and apparent grain boundary resistivity of 8YSZ reference, compared with total resistivity of the best samples from the three powder suppliers (after re-annealing at 1500°C)

T (°C)	reference sample 8YSZ			HR1500	MEL1500	U1500
	R_{ig}	R_{gb}	R_{tot}	R_{tot}	R_{tot}	R_{tot}
Ω .cm ²						
300	138407	65648	204055	390097	527286	1087840
400	6730	2486	9216	17204	20395	56996
500	730	224	953	1751	1889	6696
600	133	35	167	309	357	1189
700	35	8	55	83	96	267
800	11.9	2.6	22.4	28.9	33.5	79.8
900			10.8	12.1	14.1	29.6

dance spectroscopy and attributed to a different microstructure of these samples at intergranular zones.

References

1. Moens, J. and Gruner, H., Performance and production of vacuum plasma sprayed solid oxide fuel cells. In *Proceedings of the 3rd European Solid Oxide Fuel Cell Forum*, ed. Ph. Stevens, Forum Sekretariat U. Bossel, Morgenacherstr. 2F, 5452 Oberrohrdorf, Switzerland, 1998, pp. 115–123.
2. Lang, M., Franco, T., Henne, R., Schaper, S. and Schiller, G., Characterisation of plasma sprayed thin film SOFC for reduced operation temperatures. In *Proceedings of the 4th European Solid Oxide Fuel Cell Forum*, ed. A. J. McEvoy, Forum Sekretariat U. Bossel, Morgenacherstr. 2F, 5452 Oberrohrdorf, Switzerland, 2000, pp. 231–241.
3. Nagata, N., Iwasawa, C., Yamaoka, S., Seino, Y. and Ono, M., Development of self-supporting air electrode type solid oxide fuel cell. In *Proceedings of the 4th International Symposium on Solid Oxide Fuel Cells*, ed. M. Dokiya, PV95-1, The Electrochemical Society, Inc., 10 South Main St., Pennington, New Jersey 08534-2896, 1995, pp. 173–180.
4. Nagata, S., Okuo, T., Kaga, Y., Kasuga, Y., Momma, K., Tsukamoto, K. and Uchiyama, F., Development of tubular solid oxide fuel cells using metallic substrates. In *Proceedings of the 4th International Symposium on Solid Oxide Fuel Cells*, ed. M. Dokiya, PV95-1, The Electrochemical Society, Inc., 10 South Main St., Pennington, New Jersey 08534-2896, 1995, pp. 221–229.
5. Van herle, J., McEvoy, A. J. and Thampi, K. R., Conductivity measurements of various yttria-stabilized zirconia samples. *J. Mater. Sci.*, 1994, **29**, 3691–3701.
6. Bauerle, J. E., Study of solid electrolyte polarisation by a complex admittance method. *J. Phys. Chem. Solids*, 1969, **30**, 2657–2670.
7. Kilner, J. A. and Waters, C. D., The effects of dopant cation-oxygen vacancy complexes on the anion transport properties of non-stoichiometric fluorite oxides. *Solid State Ionics*, 1982, **6**, 253–259.
8. Inozemtsev, M. V. and Perfilov, M., Effect of impurities on the electrical properties of an oxide-type solid electrolyte. *Elektrokhimiya*, 1975, **11**, 1031–1036.
9. Fabry, P., Schouler, E. and Kleitz, M., Ion exchange between two solid-oxide electrolyte. *Electrochim. Acta*, 1978, **23**, 539–544.
10. Schouler, E. J. L., Masbahi, N. and Vitter, G., In situ study of the sintering process of yttria stabilized zirconia by impedance spectroscopy. *Solid State Ionics*, 1983, **9–10**, 989–996.